

Acoustic behavior of an Air Motion Transformer (AMT) Transducer

Nico Günter Germanos

Physical-Lab, nico@physical-lab.com

Rubén Picó Vila

Institut d'Investigació per a la Gestió Integrada de les Zones Costaneres (IGIC), Universitat Politècnica de València (UPV), 46730 Gandia, Spain, rpico@upv.edu.es

Francisco Castells Ramon

Instituto ITACA, Universitat Politècnica de València, Valencia 46022, Spain, fcastells@eln.upv.es

Abstract. This paper presents different approaches for examining the acoustical behavior of an Air Motion Transformer (AMT). The model was set up step by step by using a very simple acoustical 2D approach that was expanded to a 3D model. This simplification was used to simulate the directional behavior of the foil with different size parameters. A structural mechanics node was then added to examine the vibroacoustic behavior of the foil using a multiphysics acoustic-structure boundary coupling node. Finally, a magnetic field node was added to simulate the whole AMT. The coupling between the magnetic part and the structural part was solved by using the Lorentz forces of the magnetic fields interface acting on the circuit traces on the foil. In this model parameters from an existing AMT were used to compare the simulated results with the real model. The data obtained provides a deeper understanding of how size parameters of the foil with the circuit traces affect the acoustical radiation of this special transducer design.

I. INTRODUCTION

Oskar Heil patented the first Air Motion Transformer in 1969 during his investigations of the fundamental characteristics of human hearing [10]. Since then, this unique form of a high-frequency transducer has been used by a wide range of loudspeaker manufacturers around the world because of its very flat acoustical response and low distortion [1,2,3]. As the foil can have large dimensions, very high sound pressure levels can be achieved. Such transducers have also been used for large line arrays in public address loudspeakers. The difference between the AMT and common tweeters is that the AMT does not use a coil in a magnetic gap like a regular transducer. Instead a folded foil from a flexible material is used onto which aluminum circuit traces are bonded. This circuit is designed so that the opposing surfaces of the foil move towards each other and thus build up acoustic pressure from the Lorentz forces of the circuit in the magnetic field.

This paper uses numerical methods, calculated by COMSOL version 6.3, to simulate the acoustic radiation of the foil geometry as well as the electromagnetic behavior of the motor system of the transducer.

As the 3D model, based on a real AMT and modeled with SolidWorks, had many details and no symmetry a lot of simplifications were made as the high-fidelity model was not solvable due to a high amount of DOFs (degrees of freedom) resulting in extremely high computational costs.

The work started as simply as possible with an acoustical 2D model of the foil to find out how the directivity pattern changes with different sizes of the foil geometry. Afterwards this model was extended to an acoustical 3D model to analyze the horizontal as well as the vertical radiation pattern with changing sizes of the geometry.

In the next step a structural mechanics shell node was added as well as the materials of the AMT. In this study, the geometry data of a real AMT were used to make the results between the simulation and the real transducer comparable. As this study is using a fixed force for the circuit on the foil, data was collected by simulating the B-field with the sizes of the magnet system of the real AMT. Using simple approximations, a fixed body load was calculated by hand using the simulated B-field data and the length of the real coil. This result was taken as an initial force for the acoustic-structure node.

Afterwards the results of the magnetic fields node with a coil were coupled to the structural shell part using the numerically calculated Lorentz force. These results were then coupled to the acoustics node where the displacement of the foil caused by the Lorentz force in the circuit produces an acoustic pressure.

All these steps combined provide deeper insight into how an AMT transducer is working. This might be useful for further investigations and developments of these kinds of interesting transducers.

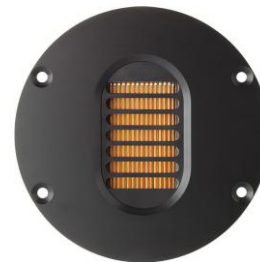


Figure 1: Picture of an Air Motion Transformer

This paper is divided into several sections. Section 3 describes the materials and methods. The geometry as well as the meshing techniques and the solver settings are explained. Section 2 will explain the theory behind the AMT and section 4 will show the results obtained from COMSOL with an additional discussion. Section 5 explains the concluding remarks.

II. Theory

A. Transducer principle

An AMT tweeter is basically constructed as shown in Figure 1.

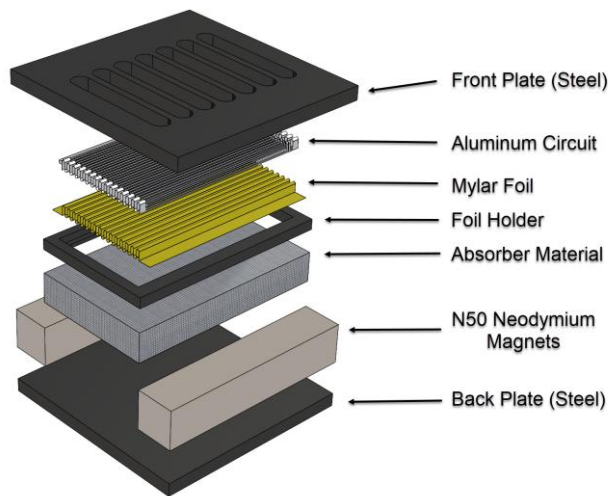


Figure 2: SolidWorks exploded view of the remodeled AMT

The neodymium magnets combined with the front- and back plates form the magnetic motor system of the transducer. The magnetic field and the current flow direction are interacting when a voltage or current is applied to the circuit. The resulting Lorentz force [5] is the force exerted on a charged particle by electric and magnetic fields. The resulting force can be written as

$$F_l = B \cdot L \cdot I \cdot \sin\alpha \quad (1)$$

where B is the magnetic field, L the length of the coil or wire and I the current. $\sin(\alpha)$ is the angle between the current flow and the B-field. The force reaches its maximum when the flow and the field are perpendicular as $\sin(90) = 1$. The aluminum conductor is folded along the foil like a rectangle function. After the first pass, the conductor is guided backwards around

the entire foil to maximize the conductor's length and thereby increase the force.

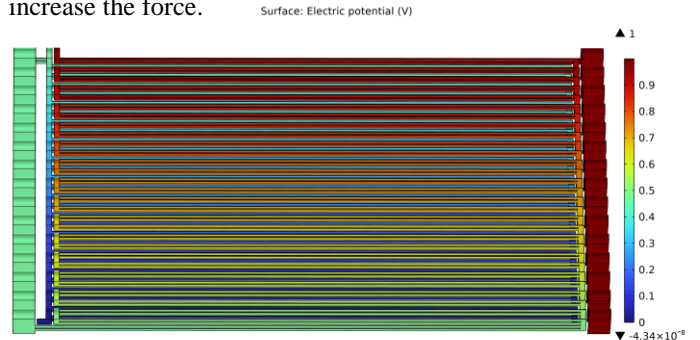


Figure 3: Electrical potential of the aluminum circuit shows the back and forth winding of the conductor along the foil

This folding leads to forces on the faces of the foil that act in opposite directions.

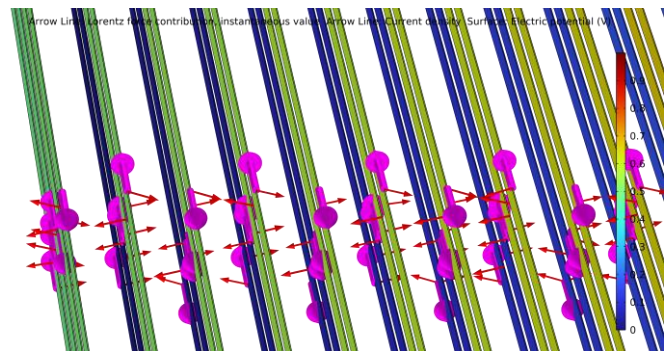


Figure 4: Current direction and Lorentz forces on the circuit traces.

The average Lorentz force for the vibroacoustic model was calculated using formula (1). Therefore, the average B-field was simulated and the length of the circuit was measured on the detached AMT.

B. Physics Interfaces

In this section the physics behind the interfaces and conditions will be presented. The **pressure acoustics interface** offers a wide range of options for solving different problems. In the frequency domain study, the Helmholtz equation [6]

$$\nabla \cdot \left(-\frac{1}{\rho} (\nabla p_t - \mathbf{q}_d) \right) - \frac{k_{eq}^2 p_t}{\rho} = Q_m \quad (2)$$

is solved for the pressure

$$p(\mathbf{x}) = p(x, y) \cdot e^{-ikx} \quad (3)$$

where ρ_t is the density of the medium (in this case air), p_t the total pressure (including background pressure) and the wavenumber k . Q_m describes a monopole source whereas q_d represents a dipole source.

The normal acceleration node adds a normal acceleration on an interior boundary. This node can be used to model movements from different kinds of sources. The condition can mathematically be described as:

$$-\mathbf{n} \cdot \left(-\frac{1}{\rho_c} (\nabla p_t - \mathbf{q}_d) \right)_{Up/Down} = -a_n \quad (4)$$

That means that this condition is adding the normal part of an acceleration to this boundary. The porous domain condition describes a porous medium with a defined damping. In this study the empirical Delany-Bazley model was chosen. This condition solves for equation (2), but with a different c in the wavenumber formulation [7]:

$$k_{eq}^2 = \left(\frac{\omega}{c_c} \right)^2 \text{ with } c_c = \frac{c}{(1+c_1X^{-c_2}-ic_{13}X^{-c_4})} \text{ and } X = \rho_f \frac{f}{R_f}$$

In these studies, the flow resistivity R_f was set to $8000 \frac{Pa \cdot s}{m^2}$ by a user definition. The exterior field calculation boundary adds the ability to compute the pressure field and phase at any point outside the defined domain. This can be achieved by solving for the Helmholtz-Kirchhoff integral. In short this presupposes that the sound pressure is determined within a volume free of sources, if sound pressure and velocity are determined in all points on its surface [8]. The interior sound hard boundary conditions can be used, for example, for walls that are reflective. Here the normal component of the acceleration is set to 0. This is applied on the upper and lower sides of the boundary.

$$-\mathbf{n} \cdot \left(-\frac{1}{\rho_c} (\nabla p_t - \mathbf{q}_d) \right)_{Up/Down} = 0 \quad (5)$$

The symmetry boundary condition can be used if symmetry can be applied on the model to reduce elements and thus number of DOFs. This is highly recommended when dealing with bigger models like the vibroacoustic model or the full electroacoustic model. The computational time saving can be immense.

The symmetry is calculated as:

$$-\mathbf{n} \cdot \left(-\frac{1}{\rho_c} (\nabla p_t - \mathbf{q}_d) \right) = 0 \quad (6)$$

As can be seen formula (5) and (6) are nearly the same. The only difference is that it is just applied on one side instead of both. The **structural mechanics interface** with a linear elastic material is used to model the moving parts of the AMT. As the foil with the circuit traces is very thin the shell interface was chosen. Shells can be modeled as boundaries, and the

kinematics in the transverse direction is represented only by the mathematical model (thickness must be specified in the shell node thickness and offset). This can be used with structures where in-plane dimensions are much larger than the thickness. This feature is very useful when dealing with very thin structures that are complicated to model and mesh. This also saves a lot of elements and computational time. This interface primarily solves for the displacements and rotations of the shell's midplane, considering its bending stiffness and deformation. Essentially, it allows one to analyze how these structures behave under various loads and boundary conditions, like stress, strain, and deformation. The dependent variables solved for in 3 dimensions are the displacements u , v , and w in the global x , y , and z directions, and the displacements of the shell normals a_x , a_y , and a_z in the global x , y , and z directions.

A body load condition was applied on the vibroacoustic and the full electroacoustic model. The vibroacoustic model uses a total force value and for the electroacoustic model a force per deformed volume was chosen with the Lorentz forces from the magnetic fields interface to couple both interfaces. Fixed constraints were also used to fix the edges and boundaries were needed. This represents the glue used in the real AMT. That means that the displacements and rotations are 0 in all directions.

$$\mathbf{u} = \mathbf{0}; \mathbf{ar} = \mathbf{0} \quad (7)$$

The symmetry boundary condition was also applied on the models where \mathbf{e}_n is the normal vector.

$$\mathbf{u} \cdot \mathbf{e}_n = \mathbf{0}; \mathbf{ar} \cdot \mathbf{e}_n = \mathbf{0} \quad (8)$$

The magnetic fields and the Lorentz forces were calculated with the **magnetic fields interface**. This interface is solving for the Maxwell equations [9]. In this node two Ampère's law in solids conditions were used to model the soft iron with losses and the N52 neodymium parts of the motor. Whereas a B-H curve as magnetization model was chosen for the iron

$$\mathbf{B} = f(\|\mathbf{H}\|) \frac{\mathbf{H}}{\|\mathbf{H}\|} \quad (9)$$

where \mathbf{B} and \mathbf{H} are the field vectors a remanent flux density formulation with a defined direction was chosen for the neodymium:

$$\mathbf{B} = \mu_0 \mu_{rec} \mathbf{H} + \|\mathbf{B}_r\| \frac{\mathbf{e}}{\|\mathbf{e}\|} \quad (10)$$

As well as in the other interfaces a symmetry condition was added. Here the symmetry guarantees the symmetry of the flux density. This is calculated as

$$\mathbf{n} \cdot \mathbf{B} = \mathbf{0} \quad (11)$$

Where \mathbf{n} is the normal vector and \mathbf{B} the field vector. The last node is the coil node. This condition was applied to model the aluminum circuit traces on the foil. This condition is handled

like an external applied current or voltage. This node solves for

$$J = \sigma E \quad (12)$$

where J is the current density and E the electric field. The inputs and outputs of the conductor were determined in the coil node.

III. MATERIALS AND METHODS

As mentioned in the introduction the model was set up in COMSOL version 6.3. Four different models were created, ranging from a simple 2D acoustic simulation to a full 3D multiphysics model. Each of the models is explained in the following.

A. Simple 2D acoustical model

A1. Model geometry

The first approach was made using a simple model with the parameter r (radius) and H (length) for the foil. Different sizes for r and H were chosen to simulate the sound radiation of different configurations and study their effect on the radiation pattern. The parametric sweep for the radius was set in the range of 0.3 / 0.4 / 0.5 / 0.6 / 1 and 1.5mm. The height H was calculated for the values 1 / 1.5 / 2 and 2.5mm

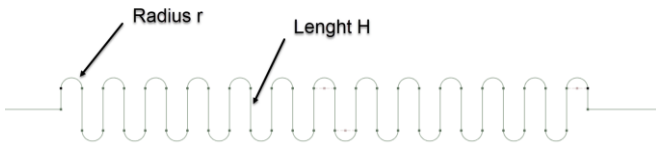


Figure 5: 2D CAD design of the foil

A sphere with a PML (perfectly matched layer) was built around the foil. The foil was then connected with the sphere like in a 2π test environment.

A2. Model materials

In this model air was used for all domains.

A3. Model mesh

The mesh was made by the user-controlled interface. It is recommended to use a maximum size of

$$\lambda = \frac{c}{5 \cdot f_{\max}} \quad (1)$$

where λ is the wavelength, c the speed of sound and f_{\max} the maximum frequency (20kHz), to achieve a good resolution of the simulation with minimum computational costs. This results in a maximum size of 0.0034m for an element. For the PML a mapped mesh with a distribution was chosen. The rest was simply meshed with free triangular elements.

A4. Physics interfaces

In this simple model just the pressure acoustics interface was used. The following physical conditions were applied to represent the model:

- **Interior Normal Acceleration:** This condition was applied on the length elements in the foil geometry. The value was set to $100 \frac{m}{s^2}$. The acceleration was set up so that the parts of the coil are accelerating to each other pairwise like an accordion.
- **Interior Sound Hard Boundary:** This condition was applied on the parts of the foil with radius r and the line that is splitting the air domain to a 2π domain.
- **Exterior Field Calculation:** This condition was applied on the boundaries of the inner sphere. Using this node COMSOL is able to compute the far field around the whole model using a full integral with the SPL and phase data inside the air domain. An additional symmetric/sound hard boundary in the x -plane was chosen to ensure a result like a 2π measurement [4].
- **PML Layer:** This layer is used to dampen the sound pressure in a very effective way to prevent reflections of the waves from the air domain edges. This technique acts like an infinite air domain without interaction of any obstacles.

A5. Study setup

A frequency domain study using an ISO preferred range from 1 kHz to 20 kHz with 1/6-octave resolution was chosen. As the model has few DOFs (degrees of freedom) the frequency domain simulation is quite effective and fast. A parametric sweep with different length and height sizes was also applied. The model was computed using the standard solver.

B. Simple 3D acoustical model

B1. Model geometry

For the second approach the geometry of the foil was just expanded in the third dimension. A small back chamber with an absorbing material was also added. To reduce the amount of DOF's the whole model was quartered and two symmetry conditions were applied to minimize computational time. Figure 6 shows the geometry.

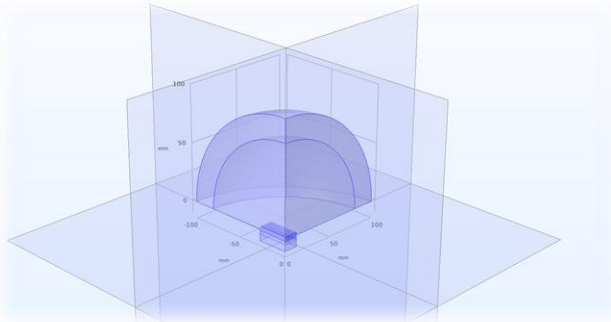


Figure 6: Quartered model with back chamber

The length and the height and the chamber with the absorbing material were parameterized to solve for different sizes of r (0,25 mm / 0,5 mm and 1 mm) and H (1 mm / 2 mm and 3 mm) as well as for the overall length l (54 mm and 108 mm).

B2. Model materials

In this model just air was used for all domains as in the simple 2D model.

B3. Model mesh

For the PML a swept mesh with a defined distribution was chosen. For the remaining domains a free tetrahedral mesh was selected with a user-controlled size with a maximum element size of $\lambda/5$ to ensure a good resolution and to keep computational times low.

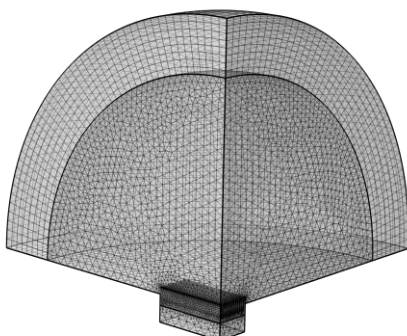


Figure 7: Mesh of the simple 3D model

B4. Physics interfaces

Here, only the pressure acoustics interface was used. The following conditions were applied:

- **Interior Normal Acceleration:** This condition was applied on the length elements in the foil geometry. The value was set to $100 \frac{m}{s^2}$. The acceleration was set up so that the parts of the coil are accelerating to each other pairwise like an accordion.
- **Interior Sound Hard Boundary:** This condition was applied on the parts of the foil with radius r and the line that is splitting the air domain to a 2π domain.
- **Exterior Field Calculation:** This condition was applied on the boundary of the inner quarter sphere. Additionally all three symmetry planes for the x , y , and z coordinates were chosen as symmetric/sound hard boundaries. This way the whole model can be calculated like a full 3D model.
- **Porocooustics:** In this condition a user defined flow resistivity ($8000 \frac{Pa \cdot s}{m^2}$) with a Delany-Bazley model was used to simulate a material with acoustical damping as used in many high frequency transducers with back chambers.
- **PML-Layer:** This layer is used to dampen the sound pressure in a very effective way to prevent reflections of the waves from the air domain edges. This technique acts like an infinite air domain without interaction of any obstacles.
- **Symmetry:** Here two symmetry conditions were applied on both sides to ensure the calculations are valid for the whole 3D model.

B5. Study setup

The same study settings were used as in the simple 2D model. Here also an ISO preferred range from 1kHz to 20kHz with a resolution of $\frac{1}{6}$ octave was chosen in the frequency domain. A parametric sweep with different length and height sizes was also applied. The model was computed using the standard solver.

C. 3D vibroacoustic model

C1. Model geometry

In this model just one symmetry condition was chosen. The back chamber was deleted and the whole magnetic system with back chamber was imported from a SolidWorks file. The sizes for the magnetic system were taken from a real AMT. Fixed parameters for the radius $r = 0,5\text{mm}$ and $H = 1\text{mm}$ were selected, as these parameters also fit with the real AMT transducer. In this model aluminum boundaries were added on the foil to simulate the circuit in a simplified way.

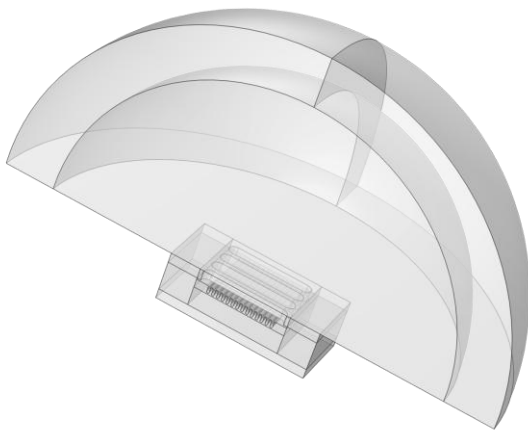


Figure 8: 3D model with fixed parameters and the magnetic system. Just a single symmetry plane was defined.

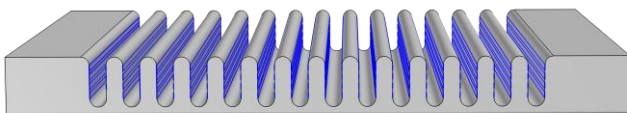


Figure 9: Simplified boundary circuit design with 4 circuit traces on each foil length H

C2. Model materials

As this is a vibroacoustic model all the structural parts needed to be defined as materials with their specific material parameters.

- **Air:** Air was chosen for all domains where no other materials were applied. This means the open space, the back chamber, the porous material and the front chamber of the foil.
- **N52 Neodymium:** This material was selected for the magnets.
- **Soft Iron with losses:** This material was chosen for the back-plate and the front-plate.
- **Aluminum:** This material was applied on the circuit traces on the foil boundary.

- **Mylar:** This material was chosen for the rest of the foil geometry. As this is not a standard material of the COMSOL library, typical parameters were used for a foil thickness of $0,02\text{mm}$.

C3. Model mesh

Like in the simple 3D acoustic model a swept mesh with a defined distribution was chosen for the PML. A free tetrahedral mesh with a predefined physics controlled normal size was then selected. As the foil is now simulated as a shell a quite fine mesh is needed to recreate the curves from the foil geometry. A tetrahedral mesh with a user defined size node was selected. The maximum element size was set to $\lambda/5$ and the minimum size was set to 0.4mm to provide a good resolution with an acceptable amount of elements to keep computational times as low as possible.

C4. Physics interfaces

In this simulation the model was expanded with a structural mechanics shell node as well as a magnetic fields node. The acoustic node and the shell node were coupled using a predefined multiphysics acoustic-structure boundary node. The magnetic fields node was not coupled to the structural mechanics shell node in this model. The magnetic fields interface was used to calculate the B-field to see how the field lines run between the front plate / back plate of the motor system of the transducer.

Setup for the acoustic interface:

This interface was chosen for the outer air domain, the PML, the back chamber with the porous material and the front chamber in front of the foil boundary.

- **Exterior Field Calculation:** This condition was applied on the boundary of the inner half sphere. Additionally, two symmetry planes for the x and z coordinates were chosen as symmetric/sound hard boundaries. This way the whole model can be calculated like a full 3D model.
- **Poroacoustics:** In this condition a user defined flow resistivity ($8000 \frac{\text{Pa}\cdot\text{s}}{\text{m}^2}$) with a Delany-Bazley model was used to simulate a material with acoustical damping as used in many high frequency transducers with back chambers.
- **PML-Layer:** This layer is used to dampen the sound pressure in a very effective way to prevent reflections of the waves from the air domain edges. This technique acts like an



infinite air domain without interaction of any obstacles.

- **Symmetry:** Here a single symmetry condition was applied to ensure that the calculations are valid for the whole 3D model

Setup for the structural mechanics shell interface:

This node was just applied on the foil boundary with the circuit traces.

- **Body Load 1 and 2:** A defined total force was applied on the circuit boundaries. Body Load 1 applies a force F_0 on every second circuit trace of a foil length and Body load 2 with a force of $-F_0$ on every second circuit trace to ensure that the circuit boundaries are moving towards each other like an accordion. This is necessary to produce sound pressure resulting from the displacement of the circuit traces and the foil.
- **Fixed Constraint 1 and 2:** The foil with the traces is fixed at the sides to prevent movement. A second constraint was used to fix all the edges on the foil as the foil was glued on the real AMT.
- **Symmetry:** Here one symmetry condition was applied on the edges of the foil boundary only.

Setup for the magnetic fields interface

In this node the neodymium magnets, the soft iron and the air domains of the front- and rear chamber were selected to visualize the B-field.

- **Ampère's Law in Solids 1:** Here the soft iron was defined by using the B-H curve selection for the magnetization model.
- **Ampère's Law in Solids 2:** A remanent flux density model was used with a flux in z-direction to define the N52 neodymium magnets.
- **Symmetry:** A symmetry plane was also applied in the magnetic fields interface

C5. Study setup

Three studies were applied on this model:

- **Vibroacoustic Study:** in this study node the coupled structural mechanics shell interface with the pressure acoustic interface was calculated in the frequency domain using an ISO preferred range from 0,5 kHz to 20 kHz with a resolution of $\frac{1}{6}$ octave.
- **Eigenfrequency:** The first 30 eigenfrequencies of the shell (foil) starting from 500 Hz were

calculated in this study. This study is only solving for the shell node.

- **Magnetic Study:** The B-field of the magnetic system was simulated using a stationary study just for the magnetic fields node.

D. 3D electroacoustic model

D1. Model geometry

This model is in principle the same as the vibroacoustic model. Due to the higher amount of DOFs a second symmetry plane was added so that the model was solved as a quarter instead of the full model.

D2. Model materials

The materials were kept the same as in the vibroacoustic model.

D3. Model mesh

The mesh is also the same as in the vibroacoustic model.

D4. Physics interfaces

In this model the magnetic fields interface was coupled to the structural mechanics shell interface. The circuit traces on the foil were modeled as a coil with input and output terminals. The Lorentz force was used as a boundary body load in the shell interface.

Setup for the acoustic interface:

The setup for the pressure acoustics interface is basically the same as in the vibroacoustic model. The only difference is that a second symmetry plane was added as well as a third axis for the exterior field calculation.

Setup for the structural mechanics shell interface:

The setup for the shell is also the same as in the vibroacoustic model. The difference here is a new body load node. Here the Lorentz force is used from the magnetic fields interface as a user-defined force per deformed volume. A second symmetry axis was also chosen.

The conditions of the vibroacoustic model were kept. A second symmetry plane was added. In this model a coil was added to couple the magnetic fields interface with the shell.

- **Coil 1:** The coil was modeled as a boundary coil condition as the foil and the circuit are modeled as a boundary plane to keep the model simple and solvable. A full 3D model with such tiny curved surfaces and thin layers will result in an extremely high amount of DOF's. Moreover, the meshing is very complex and difficult for tiny structures. The thickness of the circuit was set to 0,02 mm. The inputs and outputs of the circuit were defined in the geometry analysis node as edges. This ensures the correct flow of the current. The coil length multiplication factor was set to 2 as the coils are halved in length by a symmetry plane.

D5. Study setup

Two studies were applied on this model. The first study is a frequency domain study used for another simulation of the vibroacoustic model. The difference here is the resolution of $\frac{1}{12}$ octave in the ISO preferred range from 0,5kHz to 20kHz to make the model comparable.

The second study was set up differently to save computational time as one has to solve for 1.8 million degrees of freedom. This time a perturbed frequency domain study was chosen.

- **Step 1: Coil Geometry Analysis:** The first study step is coil geometry analysis to simulate the current flow in the circuit traces. Just the magnetic fields node was selected.
- **Step 2: Stationary Study:** In this study step a stationary study was solved for the magnetic fields interface to calculate the fields of the magnet system. Here also just the magnetic fields node was selected.
- **Step 3: Frequency Domain Perturbation:** This study was chosen to calculate the full model. A liner operator was used as initial voltage allowing for calculating around small perturbations. A $\frac{1}{12}$ octave-band spacing was chosen for the frequency sweep.

E. External data

A real AMT was measured and remodeled in SolidWorks to compare the results. The measurements were made in a big baffle (6 m x 6 m in size) to achieve reflection-free half-plane (2π) conditions like in the simulation. The applied voltage was 2,82 V. The measurement distance was 1 m. A logarithmic chirp with high resolution was used as a measurement signal. The result was smoothed

using $\frac{1}{6}$ octave-band smoothing. Afterwards the AMT was deconstructed to examine the unit and to determine the dimensions of the materials.

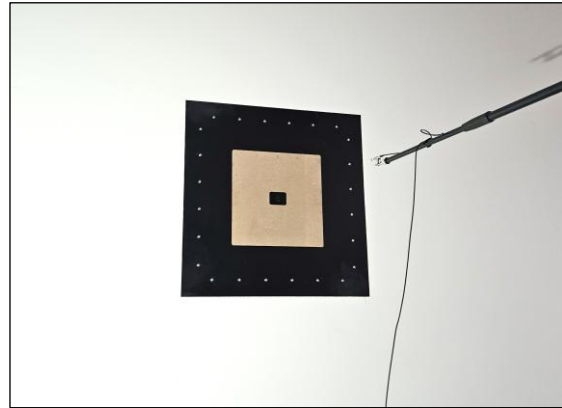


Figure 10: Experimental setup with the AMT mounted on a 6m x 6m Baffle. Measurement distance = 1 m

The neodymium magnets were considered to have a N52 grade. The thicknesses of the foil and the aluminum traces were considered to be 0.02 mm.

IV. RESULTS AND DISCUSSION

As mentioned before the final model was achieved by starting from a simple 2D model that helped to get a first insight of how different geometry parameters (radius r and length of the foil faces H ; see Figure (5)) affect the acoustic radiation pattern of the foil. Afterwards this model was enhanced to an acoustic 3D model with a length l as an additional parameter in the third dimension. This model provides a good understanding of how the directivity changes in the horizontal as well as in the vertical plane with different geometry parameters. **Appendix A** shows the directivity plots with different sizes of the parameters of the acoustic 3D model.

A. Vibroacoustic model

Before the vibroacoustic model was calculated, the magnet system was solved in the magnetic fields interface in a stationary study to obtain data for the B-field. This data was used to estimate a realistic force that was applied on the circuit traces. The average magnetic flux in the circuit plane was determined to be 0.34 T (Figure 11 and 12). The length of the coil was measured to be 70cm. The current was set to 0.5 A. Using equation (1) gives a result of around 0.12 N when the field is considered perpendicular to the current direction. As this ideal assumption is not fully valid, as seen in the magnetic flux plot in Figure (13), a loss of 20% was deducted (resulting in 0.1 N) as the B-field lines are not perpendicular in the area

of the neodymium magnets in the motor. This value was used as the body force load on the aluminum circuit traces.

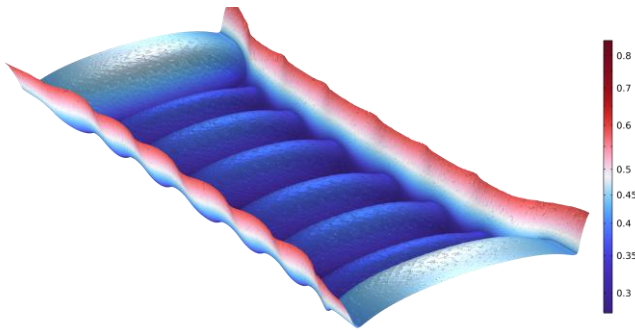


Figure 11: Profile of the magnetic flux density inside the magnet system. A cut plane through the circuit was used to calculate the flux at the circuit position. One can see the holes from the front plate that are affecting the flux profile

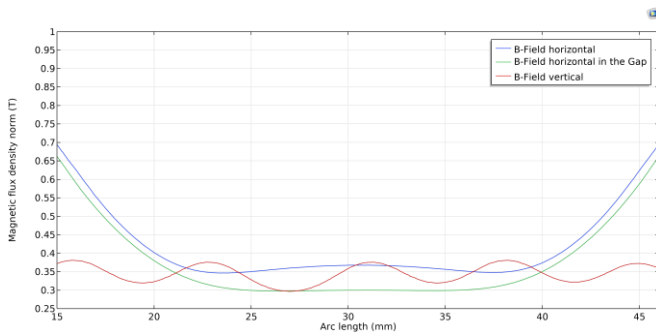


Figure 12: Flux density in the circuit plane in horizontal and vertical direction. 2 horizontal sets were calculated in the horizontal plane as the front plate has holes.

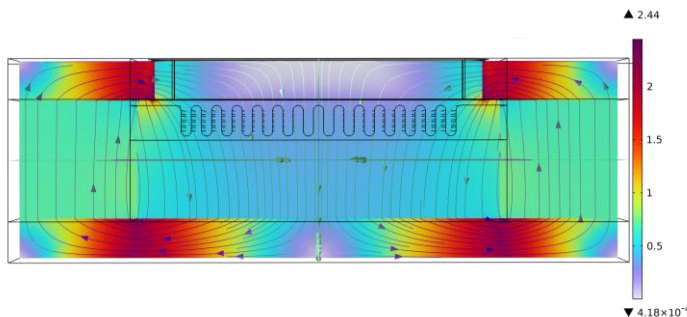


Figure 13: Flux density profile in the horizontal plane with a max of 2.44T

After the magnetic fields study an Eigenfrequency study was calculated to examine the behavior of the foil and to locate the first eigenmodes. Figure (14) shows the first six eigenmodes of the foil with the aluminum circuit traces.

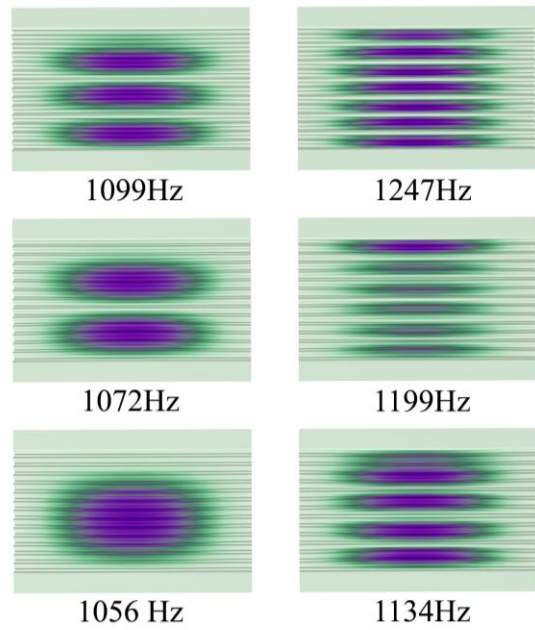


Figure (14): First six eigenmodes of the foil and circuit traces

Figure (15) and Figure (16) are showing the directivity plots of the vibroacoustic model calculated at a distance of 1m.

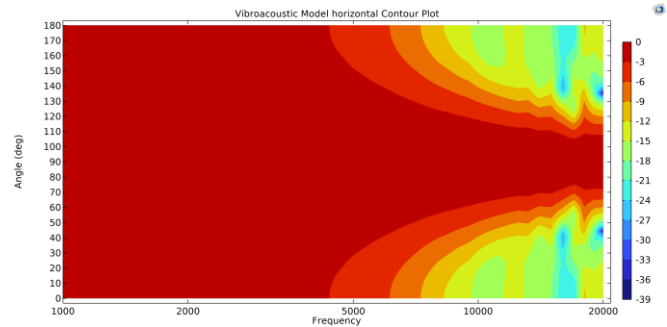


Figure (15): Horizontal polar plot of the vibroacoustic model

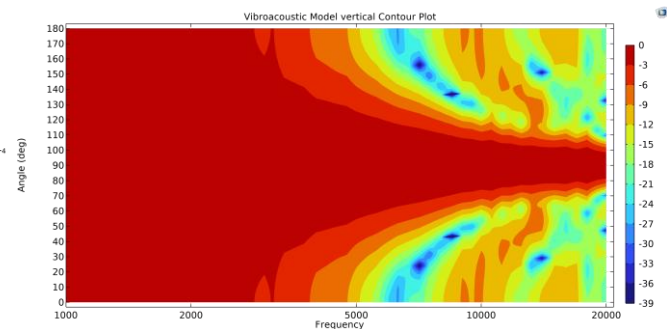


Figure (16): Vertical polar plot of the vibroacoustic model

B. Electroacoustic model

In this model the magnetic fields interface was coupled with the structural mechanics shell interface using the Lorentz force to drive the aluminum circuit traces. Here the polar plots were also plotted to compare the results with the ones obtained from the vibroacoustic model. The results of the magnetic fields interface are the same as in the vibroacoustic model. The difference here is that the loads on the circuit traces differ. The force on the traces on the vibroacoustic model is constant over the whole area whereas the forces differ in the electroacoustic model as the B-field lines are not perpendicular over the whole area.

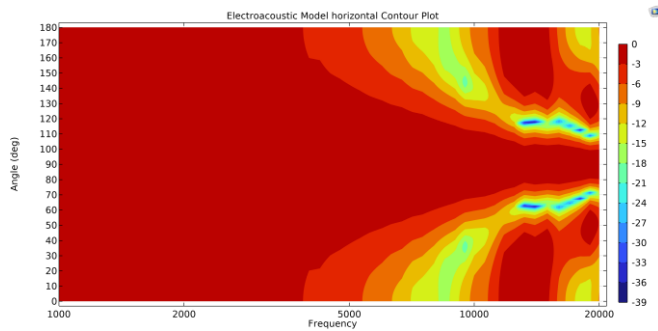


Figure (17): Horizontal polar plot of the vibroacoustic model

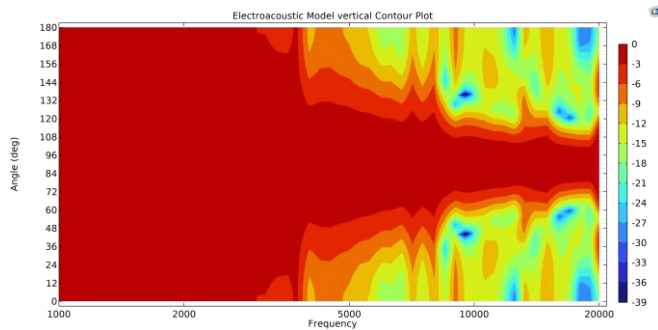


Figure (18): Vertical polar plot of the electroacoustic model

As can be seen the differences between the models are visible but small. The electroacoustic model shows a lot more details and there is a side lobe in the horizontal plot of the electroacoustic model between 12 kHz and 14 kHz.

C. Experimental AMT measurements and comparison

Here the measured data of the real AMT are presented to compare the plots. In the range from 1 kHz to 3 kHz the simulations show omnidirectional behavior. This is not the case in the real measurements. On the other hand, the results in the range from 5 kHz to 20 kHz seem to be quite close to the measurements. One should not forget that a lot of simplifications were made to keep the model size as small as possible and computational times as low as possible. For the 2D and 3D acoustic models just air was used. The geometry was built as a simple boundary with an acceleration on the faces of the foil. Afterwards the vibroacoustic model was set

up using a structural mechanics shell node to simulate the movement of the foil and circuit traces using a constant force on the circuit traces with defined material parameters. Here the magnet system and the absorbent material between the foil and the back plate of the magnet system were also defined. The electroacoustic model also considers the B-field, were not all field lines are perpendicular resulting in a Lorentz force that is not constant in the magnet system.

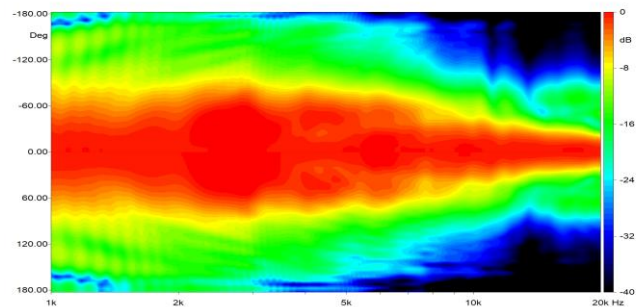


Figure (19): Horizontal polar plot of the AMT

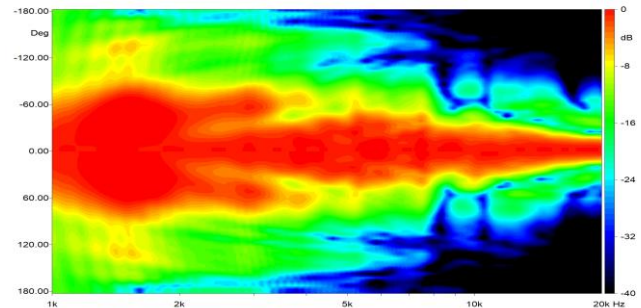


Figure (20): Vertical polar plot of the AMT

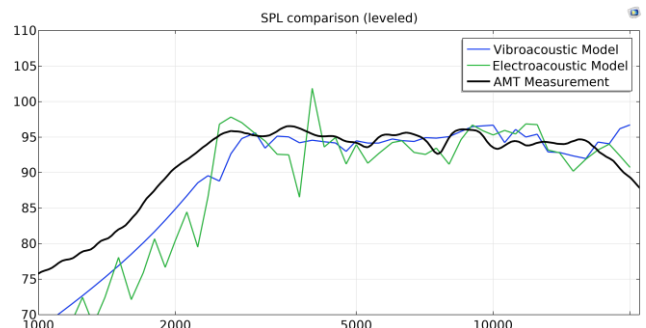


Figure (21): SPL comparison of the models with the real AMT

The differences between the models and the AMT are quite small although a lot of simplifications were made. The holder for the foil was not modeled and the parameters of the damping material were estimated. Also, the spaces between the front plate and the foil differ as small spaces were avoided to keep the number of elements small.



V. CONCLUSIONS

Modern simulation tools make it possible to get a valuable insight in the physics of complicated processes. It is even possible to isolate individual effects and only consider one parameter. This study shows that even with very simple models a lot can be investigated to identify relevant trends for the changes one is looking for. Starting with a simple model was the right choice as the physics can get complex and complicated. The gradual expansion of the model minimizes sources of error and makes simulation easier. An attempt was made to simulate the entire complex 3D model with all its details, but this failed in several places. The mesh was extremely complex and fine as the foil and the circuit shown in Figure (7) shows a lot of thin and small details. The whole model consisted of 30 million DOFs and the machine used was not able to solve the model. By simplifying the model and using symmetry, a model with 1.8 million DOFs was achieved. This is a factor of over 16 times.

The models show that the design of an AMT can be quite challenging. The sizes of the foil parameters significantly change the directional behavior as well as the SPL. Also, the holes on the front interact with the acoustic response. For further investigations different types of holes could be investigated or a shape or topology optimization could be applied to get better results. Different types of geometries could be simulated for the foil as well as different materials using a material sweep. The same applies to the magnetic system.

Regarding the results, one can say the models agree reasonably well with the real unit. The use of numerical simulations allows for deep insights into the effects of different isolated parameters. This significantly reduces the number of prototypes and development time.

ACKNOWLEDGMENTS

The authors gratefully acknowledge the technical and academic support of the Multiphysics Modeling School (<https://www.multiphysics.uma.es>).

REFERENCES

- [1] A. Muscheites, D. Leckschat, and C. Epe, "Line array sound reinforcement systems using air motion transformer", *Acta Acustica united with Acoustica*, vol. 102, no. 3, pp.592-599, 2016.
- [2] P. J. Riccardi and T. E. Blanford, "One-Dimensional modeling of the air motion transformer", *The journal of the Acoustical Society of America*, vol. 151, no.4, ppA57-*A58, 2022
- [3] D. Leckschat, A. Muscheites, and C. Epe, "Suitability of folded-ribbon high-frequency drivers for high-power sound reinforcement systems," in *Audio Engineering Society*

Conference: 59th International Conference: Sound Reinforcement Engineering and Technology, July 2015. (Online); <https://www.aes.org/e-lib/browse.cfm?elib=17833>

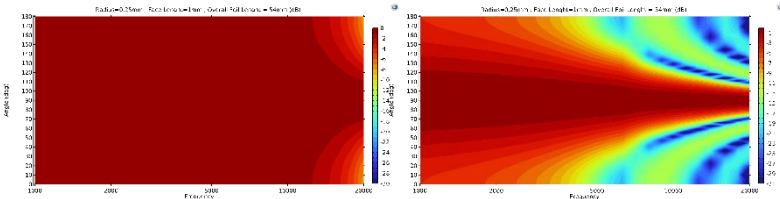
- [4] "COMSOL multiphysics reference manual 6.3" pp.2081-2085, 2025.[Online].Available:https://doc.comsol.com/6.3/doc/com.comsol.help.comsol/COMSOL_ReferenceManual.pdf
- [5] M. Kleiner, *Electroacoustics*. CRC Press, 2013
- [6] "COMSOL 6.3 The Acoustics Module User's Guide 6.3" pp.39-40,2025[Online].Available:<https://doc.comsol.com/6.3/doc/com.comsol.help.aco/AcousticsModuleUserGuide.pdf>
- [7] Cox, Trevor / D'Antonio, Peter (2016): *Acoustic Absorbers and Diffusers. Theory, Design and Application*. Boca Raton, Fla (CRC Press).
- [8] Williams, Earl G.: *Fourier Acoustics : Sound Radiation and Nearfield Acoustical Holography*. Amsterdam, Boston: Academic Press, 1999.
- [9] Jackson, John David: *Classical Electrodynamics*. New York: John Wiley & Sons, 1998
- [10] Patent US3636278: *Acoustic Transducer With A Diaphragm Forming A Plurality Of Adjacent Narrow Air Spaces Open Only At One Side With The Open Sides Of Adjacent Air Spaces Alternatingly Facing In Opposite Directions*. Veröffentlicht am 18. Januar 1972, Erfinder: Oskar Heil.



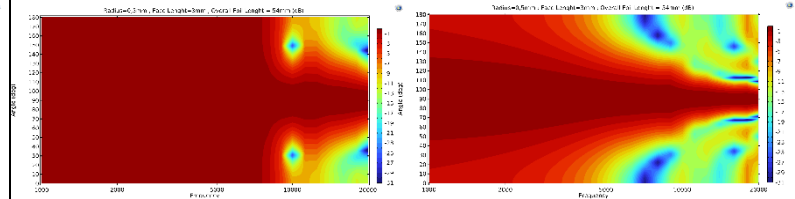
VI. Appendix

Foil overall Length: $l=54\text{mm}$

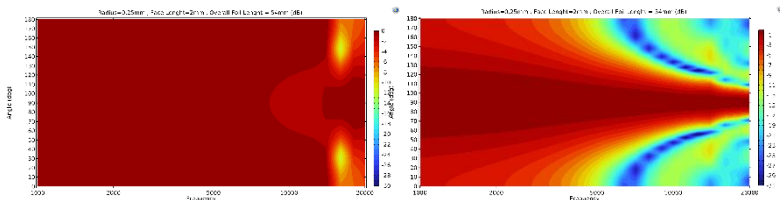
Radius $r=0,25\text{mm}$; $H=1\text{cm}$
Horizontal vertical



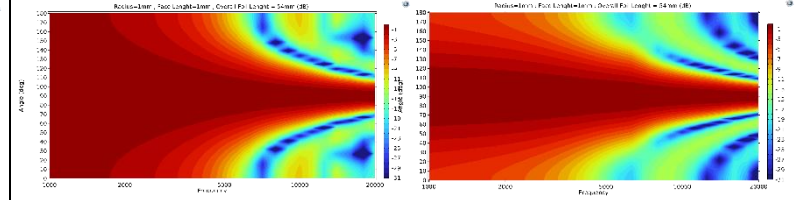
Radius $r=0,5\text{mm}$; $H=3\text{cm}$
Horizontal vertical



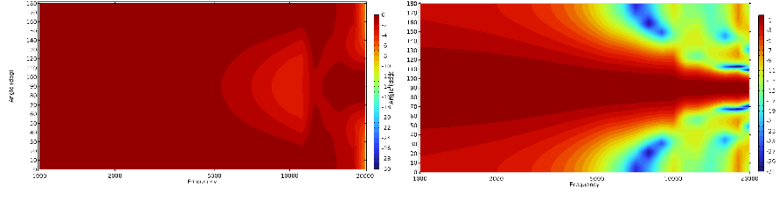
Radius $r=0,25\text{mm}$; $H=2\text{cm}$
Horizontal vertical



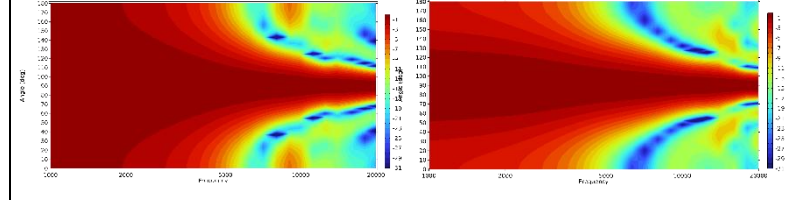
Radius $r=1\text{mm}$; $H=1\text{cm}$
Horizontal vertical



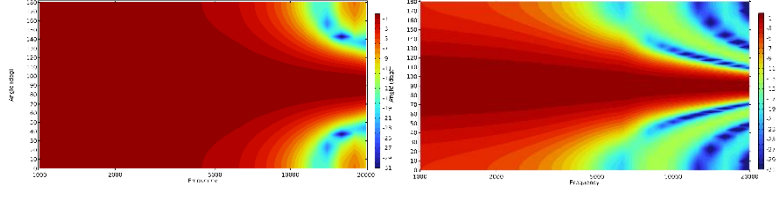
Radius $r=0,25\text{mm}$; $H=3\text{cm}$
Horizontal vertical



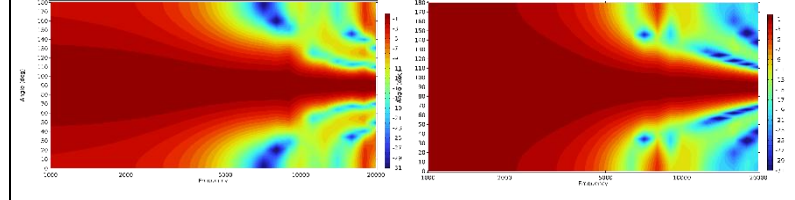
Radius $r=1\text{mm}$; $H=2\text{cm}$
Horizontal vertical



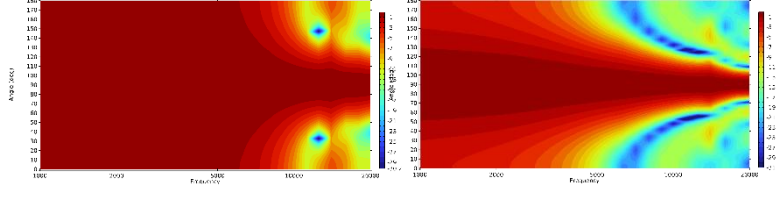
Radius $r=0,5\text{mm}$; $H=1\text{cm}$
Horizontal vertical



Radius $r=1\text{mm}$; $H=3\text{cm}$
Horizontal vertical



Radius $r=0,5\text{mm}$; $H=2\text{cm}$
Horizontal vertical



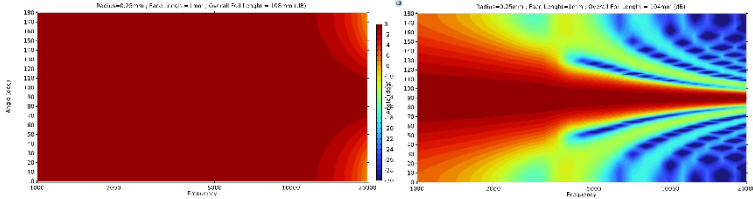


Foil overall Length: $l=108\text{mm}$

Radius $r=0,25\text{mm}$; $H=1\text{cm}$

Horizontal

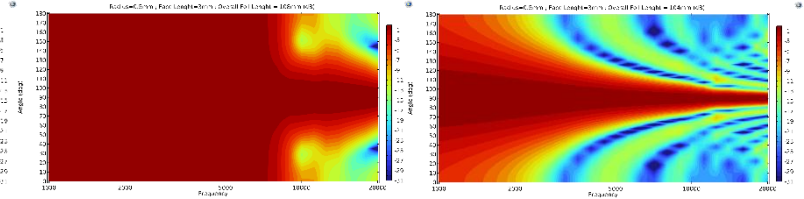
vertical



Radius $r=0,5\text{mm}$; $H=3\text{cm}$

Horizontal

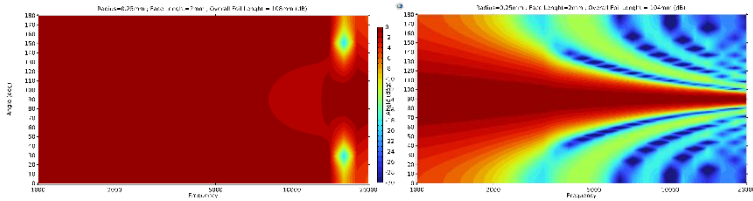
vertical



Radius $r=0,25\text{mm}$; $H=2\text{cm}$

Horizontal

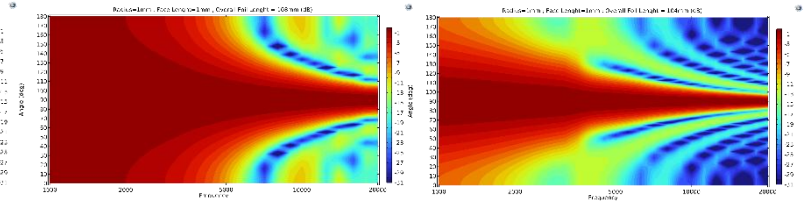
vertical



Radius $r=1\text{mm}$; $H=1\text{cm}$

Horizontal

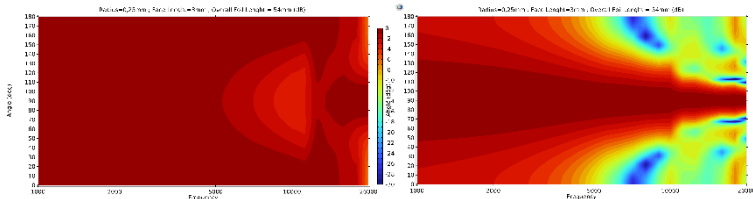
vertical



Radius $r=0,25\text{mm}$; $H=3\text{cm}$

Horizontal

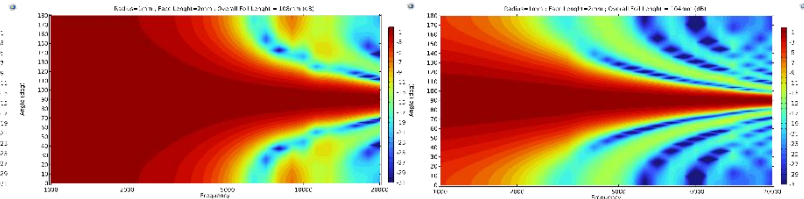
vertical



Radius $r=1\text{mm}$; $H=2\text{cm}$

Horizontal

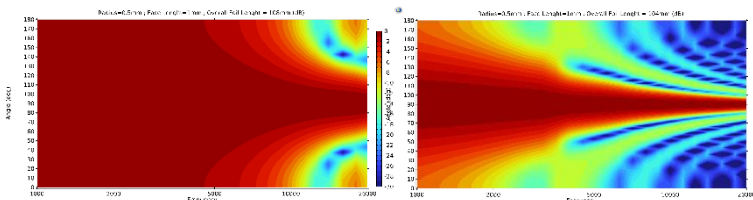
vertical



Radius $r=0,5\text{mm}$; $H=1\text{cm}$

Horizontal

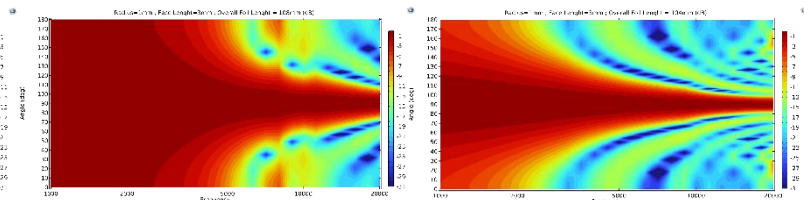
vertical



Radius $r=1\text{mm}$; $H=3\text{cm}$

Horizontal

vertical



Radius $r=0,5\text{mm}$; $H=2\text{cm}$

Horizontal

vertical

